The Nature of Wind Loads and Dynamic Response

by D. Boggs and J. Dragovich

Synopsis: The elements of dynamic response are presented. Using the model of a single degree of freedom oscillator, the nature of wind loads and their effect on dynamic response are discussed. The results of the response of a single degree of freedom oscillator are used to describe the current building code procedures. The measured damping in structures is presented and conclusions regarding the appropriate level of damping to use as a function of drift are presented. Finally, issues related to the use of load factors are highlighted.

Keywords: background; damping; dynamic response; resonance; wind loads

16 Boggs and Dragovich

Daryl Boggs is principal and vice president of Cermak Peterka Petersen, Inc., Fort Collins, Colorado. He specializes in wind-tunnel testing and consulting on wind-sensitive and dynamically active structures. He is a member of ACI 375, performance-based wind design, and a corresponding member of the ASCE 7 Task Committee on Wind Loads.

Jeff Dragovich is an assistant professor in the department of civil and environmental engineering at Seattle University. He is a member of ACI 374, performance-based seismic design, ACI 375 Performance-Based wind design. His research interests include tall building design and earthquake engineering.

INTRODUCTION

The effect of wind on a structure is three-fold. The structure must have sufficient strength to resist the wind-induced forces, the structure must have adequate stiffness to satisfy occupant comfort and serviceability criteria, and the wind may produce a dynamic response of the structure. This third effect is of particular importance in that it may amplify the first two effects. The dynamic response of structures, in particular building structures, to wind loading and the nature of the wind loads that produce this effect are the focus of this paper.

Wind is a dynamic and random phenomenon in both time and space. This is illustrated in Figure 1, which shows the measured wind speed at three elevations on a mast during an 8-minute time interval. Inspection of these records permits the following observations: first, the wind speed can be described as a mean value upon which random fluctuations or "gusts" are superimposed; secondly, this mean wind speed increases with height above the ground; and third, there is no obvious correlation between the fluctuations at the different heights. Although not obvious in Figure 1, the fluctuations are also random in time: the waveforms do not repeat, and the wind speed at any time can be described statistically but not predicted exactly. These observations are a characteristic of boundary-layer flow, and the natural winds represented by these records are referred to as the atmospheric boundary layer. It is assumed that wind speed is not affected by the presence of the mast structure.

The dynamic response of a low-rise building is likely insignificant, assuming it has been adequately designed for both strength and stiffness limits states. However, it is important to quantify the case where dynamic response may be neglected. The building's fundamental natural frequency of vibration, f_0, is the most widely accepted property of a structure used to determine whether dynamic response will be significant under wind loading. It has the added feature of being concise and commonplace in the vocabulary of a structural engineer involved in seismic design.

The ASCE Standard [ASCE 7-05] classifies a structure as dynamically sensitive, or "flexible" if $f_0 < 1$ Hz, otherwise it is considered to be "rigid." The classification used by the ASCE Standard is widely accepted as a reasonable boundary between dynamic and rigid behavior. Consequently, this paper is focused on tall and medium-height buildings

for which $f_0 < 1$ Hz, i.e. flexible buildings. Approximate rules for determining f_0 exist and will be briefly described.

Where a building is designed for reasonable drift ratio, one widely used approximate formula is

$$f_0 = 46/H \ (H = \text{building height in m})$$
$$= 150/H \ (H \text{ in ft}) \quad (1)$$

which appears to agree well with *measured* values of many buildings worldwide. However, *calculated* frequencies of buildings in the U.S. appear to be better described by

$$75/H < f_0 < 100/H \ (H \text{ in ft}) \quad (2a)$$

or, alternately as

$$75 < f_0 H < 100 \ (H \text{ in ft}) \quad (2b)$$

Equation (2b) can be inferred directly from Fig. 2, where the *y*-axis is the product of $f_0 H$. Note that if one considers a 10-foot story height, the upper bound of $100/H$ in equation (2a) is equivalent to the approximate period formula of $T = 0.1N$, used in many seismic building codes, where T is the period of vibration and N is the number of stories. The above equations imply that the calculated frequencies are typically less than the measured frequencies, thus conservatively classifying structures as flexible based on calculation. Because of this, it is recommended that equation (2a) be used as a preliminary indicator of f_0, and a possible flexible condition.

If the structure is flexible, it is essential that the designer determine the natural frequency and mode shapes of the first few modes of vibration accurately. This is typically accomplished using eigenvalue analysis routines in commercial three-dimensional finite element computer programs.

This paper is primarily concerned with dynamic structural response. Consequently the structural parameters that determine a structure's dynamic response characteristics will be summarized.

A conceptual model suitable for analysis of dynamic response is to idealize a building as a chain of lumped masses linked by beam-column elements, as shown in Fig. 3. This model has n degrees of freedom corresponding to the lateral displacement of each floor or lumped mass. It is assumed in this simplified model that the lateral displacement and rotations are uncoupled, so that the analysis may be applied separately for each.

The system may then be described by an $n \times n$ stiffness matrix $[k]$, diagonal mass matrix $[m]$, and damping matrix $[c]$. The system "input" is an n-component vector of external loads $\{P(t)\}$ derived from the wind velocity distribution, and the "output" is an n-

component displacement vector $\{x\}$, velocity vector $\{\dot{x}\}$, and acceleration vector $\{\ddot{x}\}$. The conditions of dynamic equilibrium require that

$$[m]\{\ddot{x}\}+[c]\{\dot{x}\}+[k]\{x\}=\{P(t)\} \tag{3}$$

which represents a system of *n* coupled differential equations. By using modal analysis, however, the system can be described by *n* uncoupled equations, each of the form

$$m^*\,\ddot{\xi}+c^*\,\dot{\xi}+k^*\,\xi=P^*(t) \tag{4}$$

which describe an equivalent single-degree-of-freedom (SDOF) system vibrating in a *normal* mode. The equivalent quantities are

$$\begin{aligned} m^* &= \{\phi\}^T[m]\{\phi\}=\sum m_i\phi_i^2 \\ c^* &= \{\phi\}^T[c]\{\phi\} \\ k^* &= \{\phi\}^T[k]\{\phi\}=(2\pi f_0)^2 m^* \\ P^* &= \{\phi\}^T\{P\}=\sum P_i\phi_i \end{aligned} \tag{5}$$

These are referred to as the *generalized* mass, damping, stiffness, and load, respectively. The shape function of the mode is the system eigenvector, $\{\phi\}$. The solution of the system, ξ, is related to the physical displacements by

$$\{x\}=\xi\{\phi\} \tag{6}$$

The natural frequency of the system in any mode is

$$f_0=\frac{1}{2\pi}\sqrt{\frac{k^*}{m^*}} \tag{7}$$

The first few modes and natural frequencies of a typical building are shown in Fig. 4. The first mode is associated with the lowest frequency and smooth monotonic deformation; the higher modes feature increasing frequency and inflection points. The dominant frequency of wind gusts is relatively low compared to the lowest natural frequency of building structures, as shown in Fig. 5, and primarily excites the lowest mode of vibration. In addition, the dominant gust wavelengths are large compared to most buildings, so that the aerodynamic pressure distribution cannot conform to the higher mode shapes and is largely cancelled by the sign reversals of the higher modes in forming the generalized load. For these reasons, it is usually necessary to consider only the lowest mode of vibration when considering dynamic response to wind, although this applies separately to each of three components of response (sway in the *x* and *y* directions and twist about the vertical *z* axis). This is in contrast to dynamic response to earthquakes,

where the dominant excitation energy is in the frequency range of low-rise buildings or the higher modes of tall buildings, is applied at only a single point (the ground) rather than distributed over their height, and therefore a large number of modes must generally be considered.

NATURE OF WIND LOADS AND DYNAMIC RESPONSE

The basic dynamic response of an SDOF system is illustrated in Fig. 6. Part *a* shows the mechanical idealization excited by the aerodynamic load $P(t)$. Part *b* shows this external load is balanced by the internal spring force, damping force, and inertial force. The internal spring force may be regarded as the *static-equivalent* load, for applying this load statically to the system would result in the same spring force. Given this load, the structural engineer could design the spring without knowledge of the detailed dynamic response. This internal "response" load is the focus of this section. What follows is intended to convey the essential mathematical characteristics of dynamic response to wind loading in mathematical terms, although no attempt is made to be rigorous.

If the excitation of the SDOF system is sinusoidal, i.e., with the equation of motion

$$m\ddot{x} + c\dot{x} + kx = P_0 \sin 2\pi ft \tag{8}$$

then the steady-state solution (after any initial transients have decayed) is $x(t) = x_0 \sin(2\pi ft - \psi)$, where the instantaneous amplitude is well known to be

$$x(t) = \frac{P(t)/k}{\sqrt{\left[1 - \left(\frac{f}{f_0}\right)^2\right]^2 + \left[2\zeta \frac{f}{f_0}\right]^2}} \tag{9}$$

The magnitude of the internal response force, then, is conveniently expressed as

$$\mathbf{P} = |H(f)|P \tag{10}$$

where

$$|H(f)|^2 = \frac{1}{\left[1 - \left(\frac{f}{f_0}\right)^2\right]^2 + \left[2\zeta \frac{f}{f_0}\right]^2} \tag{11}$$

is generally regarded as the *mechanical admittance*.

Two significant observations are embedded in the above equations. First, the internal response load relative to the external applied load depends *only* on the natural frequency

and damping, as opposed to the mass or stiffness separately. Second, the ratio defined by $|H(f)|$ is a non-dimensional function that applies equally well to *any* input and output parameters linearly related to the load, and it is convenient to write the output (response) quantity as a boldface version of the input (excitation) quantity. We could also write, for example,

$$\mathbf{x} = |H(f)|x \tag{12}$$

where x would be the displacement under static application of the load P, and $\mathbf{x}$ is the dynamic displacement.

The character of $|H(f)|$ is illustrated in Fig. 7. If the exciting frequency f is close to the natural frequency f_0 and the damping is low, the function is an amplification factor describing a condition known as resonance. This always occurs to some extent in a flexible building under wind loading.

Wind excitation is not sinusoidal, but a spectrum consisting of a random superposition of a broad range of frequencies. The mean square spectral density of the response is obtained by weighting the mean square spectral density of the excitation by the mechanical admittance:

$$S_{\mathbf{P}}(f) = |H(f)|^2 S_P(f) \tag{13}$$

In the remainder of this paper, a mean square spectral density is simply referred to as a spectrum. Characteristic excitation and response spectra are shown in Fig. 8.

The term “response spectrum” as used here should not be confused with its common use in earthquake engineering. In this paper it means the mean square spectral density of the time variation of some response parameter, such as displacement, static-equivalent load or moment, or static-equivalent generalized load. In earthquake engineering it refers to a description of what the response parameter’s magnitude (peak, rms, etc.) would be if the structure’s natural frequency varied over some range.

Equation (13) applies to the SDOF system; however, it applies equally to one mode of a practical building modeled as an MDOF system simply by substituting the generalized load P^* for the simple load P. The generalized response load, $\mathbf{P}^*$, is closely related to the response base moment, and with some adjustment for particular mode shapes can lead to internal response forces applicable at each floor level (Boggs and Peterka 1989). Details are not pursued here, and the asterisk designating a generalized load is omitted in the following.

It is common practice in wind engineering to consider the response load to be the superposition of two components, referred to as *background* and *resonance*. The former

refers to the quasi-static response to the fluctuating portion of the wind load that would occur if the natural frequency were extremely high (or equivalently, to wind gusts having a frequency much lower than the natural frequency), and is usually considered to be equal to the external aerodynamic load itself. The latter represents the *additional* amplification that is embedded in $|H(f)|$, and for practical purposes may be considered the dynamic response to those gusts having a duration close to the natural period of the structure. The mean square value of the fluctuating response is obtained by integrating the response spectrum:

$$\sigma_{\mathbf{P}}^2 = \int_0^\infty |H(f)|^2 S_P(f)\, df \tag{14}$$

The peak response is defined by superimposing its mean value with the root-mean-square multiplied by a peak factor. This procedure is greatly facilitated, however, by first obtaining the peak values of the background and resonant portions as follows.

Since the background response is considered to be the load itself without resonant amplification, its rms value is simply σ_P. The spectrum of the resonant portion is then

$$S_{\mathbf{P},R}(f) = S_{\mathbf{P}}(f) - S_P(f) \tag{15}$$

as indicated in Fig. 8. The rms value of the resonant portion is therefore

$$\sigma_{\mathbf{P},R} = \sqrt{\sigma_{\mathbf{P}}^2 - \sigma_P^2} \tag{16}$$

Under particular yet common conditions this can be represented by the well-know *white noise approximation*, avoiding the integration indicated in Eq. (14):

$$\sigma_{\mathbf{P},R} \approx \sqrt{\frac{\pi}{4\zeta} f_0 S_P(f_0)} \tag{17}$$

The peak value of the fluctuating response is now found by combining the background and resonant peaks using mean square addition, and adding the mean response:

$$\hat{\mathbf{P}} = \overline{P} \pm \sqrt{(g_0\sigma_P)^2 + (g_1\sigma_{\mathbf{P},R})^2} \tag{18}$$

The peak background factor is generally taken as, approximately,

$$g_0 = 3.5 \tag{19}$$

and the peak resonance factor is generally calculated from Davenport's formula (1964)

$$g_1 = \sqrt{2\ln f_1 T} + \frac{0.577}{\sqrt{2\ln f_1 T}} \tag{20}$$

where f_1 is the natural frequency of the first mode of vibration, and T is the time period to which the peak value is referenced, generally taken as 1 hr = 3600 sec.

All current procedures for treating dynamic response of flexible buildings to wind are based on the above equations. Different approaches may be used to disguise this from the user; for example, codes and standards usually package the dynamic aspects into a simple "gust factor" or "gust response factor" to multiply the quasi-static loads that would apply if the building were rigid, and wind-tunnel methods result in equivalent-static loads that the design engineer can utilize directly in a static analysis of the structure.

Equations (17) – (20) are the basis of the dynamic gust factor as implemented in ASCE 7-05. However, the excitation spectrum $S_P(f)$ in that case is approximated on a semi-analytical basis and applies only to the along-wind load, i.e., the component of load parallel to the wind direction, which is assumed to be square-on to the face of a rectangular prismatic building. More accurate excitation spectra must be obtained from a wind-tunnel model study, as described elsewhere.

Measured spectra for the along-wind and cross-wind load components of a tall slender building are illustrated in Fig. 9. The along-wind component, within the range of frequency that affects dynamic response, monotonically decreases with frequency, indicating that the resonant portion of the response will always decrease with an increase in natural frequency. The spectrum of the cross-wind component, however, has an intermediate peak caused by vortex shedding, which could greatly affect the resonant response. Vortex shedding is a well-known phenomenon, shown schematically in Fig. 10. The vortices produce an alternating sideways force that oscillates from side to side in a nearly sinusoidal fashion. The frequency of shedding is governed by the Strouhal no., *St*, which is normally constant for a given cross-section shape with square edges, and therefore indicates that the frequency is proportional to wind speed and inversely proportional to the building width. For most buildings and design wind speeds, the shedding frequency is lower than the natural frequency of vibration, so that an increasingly lower natural frequency—i.e. reduced stiffness—results in increasingly higher response. The intensity of shedding, and therefore of the rate at which load increases with decreased stiffness, is highly dependent on the building shape and the amount of turbulence in the approaching flow. Regular symmetrical shapes and smooth flows result in more intense shedding.

The remainder of this paper considers the dynamic response of tall buildings, computed using equations (17) – (20), with the excitation spectrum measured for two orthogonal directions (*x*, *y*) from wind-tunnel tests for a full range of wind directions.

Aerodynamic loading and dynamic response in torsion can also be important in buildings. The effective eccentricity of the overall shear force is usually at least 5 to 10 percent of the building width, although it is often twice this great and in some cases it can be much higher (Boggs, Hosoya, and Cochran 2000). Torsional loading and response are not considered further here, although most of the following is conceptually applicable to torsion as well as the overturning forces.

In addition, the excitation spectrum can be, in some cases, dependent on the dynamic response of the building itself. Such a condition of "aeroelastic feedback" most commonly occurs for a tall, slender, isolated (having an open exposure) building for which the frequency of vortex shedding is close to the building's natural frequency of vibration. This condition is discussed elsewhere and is not pursued in this paper.

Wind can blow from any direction. A common misconception is that wind only needs to be considered square-on to a face of the building, and it then produces loading in the direction of that axis. In reality, the wind load in any one component direction may be governed by wind blowing from other directions. Figure 11 shows the M_x component of load as a function of wind direction through a full 360-degree range.[*] Different curves are shown for the mean, peak quasi-static (mean plus background), and peak total (mean plus background plus resonance) portions. Three total peak curves are shown, corresponding to resonance resulting from three different values of the natural frequency of vibration. The building is of medium height, has a symmetrical rectangular cross section, is relatively isolated in an otherwise open exposure with no significant neighbors, and the wind speed is assumed constant with direction.[†]

The mean load curve is approximately sinusoidal with wind direction, completing one cycle in 360 degrees. The maximum (positive or negative) values occur near 0 and 180 degrees, when the wind is perpendicular to the axis of rotation. The fluctuating background response is approximately constant with direction, as the buffeting from wind gusts occurs laterally as well as longitudinally. As a result, the peak quasi-static response (mean plus background) is still largest at 0 and 180 degrees. This is consistent with a so-called *along-wind* response, i.e., the primary loading is in the direction of the wind. This would represent the design conditions for a rigid building having a very high natural frequency. Note that the peak value is approximately twice the mean value, and the amplitude of vibration is approximately equal to the mean overall drift, or one-half of the peak overall drift.

When the dynamic response associated with resonance in a flexible building is included, this idealized picture begins to change. At most wind directions, the peak response increases modestly as the natural frequency decreases. Near 90 and 270 degrees, however, the dynamic excitation about the x axis changes from one of buffeting by

[*] The moment convention used in this paper is the right-hand rule, e.g., positive M_x is associated with base shear in the $-y$ direction.

[†] Data from figures 7, 9, and 10 were obtained from model wind-tunnel tests.

turbulence to harmonic vortex shedding. The load and response are near zero, the response is almost entirely dynamic, and the amplitude of vibration is approximately equal to the peak overall drift.

The conditions in Fig. 11 are such that shedding is unusually strong. Even at the highest natural frequency shown by the shaded circles—which is still higher than the engineer's final design value shown by the solid circles—the *cross-wind* response at 90 or 270 degrees is comparable to the *along-wind* response at 0 or 180 degrees. At his design value the cross-wind response load is about 15 percent higher. At the lowest natural frequency shown by the open circles, which is just 25 percent higher than his calculated value and therefore easily within the range of uncertainty in this value, the cross-wind load is more than 40 percent higher than the along-wind load.

Damping has an effect similar to natural frequency, as shown in Fig. 12. Increased damping will always reduce the resonant portion of the dynamic response, and it is especially effective for the cross-wind load component, just as increasing the natural frequency is effective in decreasing the resonant response. In the limit of either very high damping or very high frequency, the peak load approaches that of a rigid building.

Present building codes contain procedures for estimating the along-wind loading associated with dynamic response, but they generally cannot address the cross-wind component. Many building structures perform adequately under cross-wind loading by vortex shedding, because the magnitude of the response is, coincidentally, similar to the along-wind response. Thus the engineer may have fortuitously produced an adequate design but for the wrong reason. If the building shape and exposure conditions are prone to strong vortex shedding, it becomes ever more important for the designer to accurately predict the structure's natural frequencies, to be aware of the effects of damping, and to understand the wind mechanism that actually governs the design load—in other words, when to seek the advice of experts or a wind-tunnel study that go beyond the traditional code procedures. Moreover, an understanding of the dynamic phenomena involved will allow the engineer to effectively address the sources of excessive response and take appropriate action for improving the performance and economy of the structure.

A second important implication of the cross-wind response lies in recognizing that significant response in one component can result from *any* wind direction. This means, of course, that *all three components* can be significant at the same wind directions. Figure 13 shows the response load in three components as a function of wind direction, for a practical building in its real-world environment. At a direction of 30 degrees, the peak values of all three base moments are at or near their maximum design values. However, these loads will generally not occur simultaneously due to lack of correlation.

Figure 14 shows the joint response in M_x and M_y components of a building. Simultaneous values of the two loads have been traced over a period of time. The heavy ellipse represents a statistical envelope of the maximum excursions of the peak loads. The center of the ellipse corresponds to the mean values of each component. The ellipse could be

circular, if the two components were totally uncorrelated ($R_{xy} = 0$), or highly skewed into the corners of the bounding box if they were fully correlated ($R_{xy} = \pm 1$). The case shown represents a fairly typical condition of $R_{xy} = 0.5$. Any location along the ellipse represents a possible design condition, depending on the relative sensitivity of the structure to simultaneous loading in the two components. It is impractical to consider this continuum of cases, and five suggestions are marked. Cases 1 – 4 are based on the concept of principal-companion actions: cases 1, 2 consist of the full peak (positive, negative) values of M_x acting as the principal load, along with the companion values of M_y which are reduced somewhat from their full peak values. Load Case 5 consists of a combination in which both M_x and M_y are reduced from their full peak values, but result (in this case) in the largest vector resultant moment. Obviously, various rationales could be utilized to define various loads cases which should capture the most critical action combinations on the structure, and yet be simple enough for practical application. The issue becomes even more complex when the third component, M_z, is introduced to the combinations. Finally, the cases described above will occur at *every* wind direction—most of which will not in fact produce any governing conditions—and a final set of design load cases must be selected from all of these. Recent building codes have attempted to address the issue of load combinations in a pragmatic way. Wind-tunnel laboratories utilize various techniques to establish design load cases.

STRUCTURAL PARAMETERS, DAMPING

The preceding section has emphasized the role of the structure's dynamic properties in affecting the design loads. The fundamental properties were shown to be the natural frequency—which in turn depends on the mass and stiffness—and the damping ratio. These properties are not fixed values for any given structure, but vary according to the level of response: the natural frequency tends to decrease with increasing response, while the damping ratio increases. These trends are illustrated in Fig. 15, taken from the Japanese database of full-scale measurements (Tamura, Suda, and Sasaki 2000) (the level of response in these figures is indicated by the acceleration, as measured by instruments installed in a sample building). These trends must be addressed when considering performance-based design for a range of limit states.

In computing the natural frequencies, the designer must accurately predict the stiffness, taking due consideration for such issues as the effective width of slabs, joint flexibility, P-delta effects, cracking of concrete, and foundation flexibility. It is also important that the mass represent the sustained value that is most likely to exist at the time of the various limit-state conditions. These issues are discussed elsewhere.

There is little the engineer can do in the way of analytical prediction of the damping ratio for any particular structure. Instead, it is common to utilize estimates for various generic types of construction. It is quite common in the industry, in fact, to simply assume a critical damping ratio of 0.01 for steel frames and 0.02 for concrete frames or shear walls. This is a crude generalization and oversimplification, and in this section we examine

information from which improved estimates could be made and the implications for different limit states. In particular, the increase of damping with displacement must be addressed when considering performance-based design for a range of limit states.

All of the practical information applicable to design of building frames has been accumulated from full-scale measurements. One such survey was indicated in Fig. 15; another by Hart et al. (as reported by Blevins 1990) is summarized in Fig. 16, and another by Davenport and Hill-Carroll (1986) in Fig. 17. As in Fig. 15, the available damping data are widely scattered but are just able to demonstrate the trend of increasing with displacement, particularly with the extreme displacements of earthquake excitation. Davenport and Hill-Carroll fit a linear regression line to damping ratio vs. log normalized amplitude for various categories of building structures, including concrete structures 5 – 20 stories and concrete structures over 20 stories, as shown in Fig. 18.

There are several parameters that are responsible for the scatter in these data, and limited progress has been made in quantifying their effects. These include building height, material, and motion amplitude (which are included to some extent as parameters in most surveys), design and construction practices (e.g., Japanese vs. U.S. general practice), structural system, etc. One compilation* demonstrates convincingly that building slenderness is an important parameter, even to the extent that different damping ratios might be justified in the same building, for the two directions in rectangular building plans of high aspect ratio. Apparently lower damping is associated with buildings of greater slenderness, or in the direction of the longer axis.

Another elusive parameter responsible for some scatter is the existence of aerodynamic damping. The damping ratio ζ, to be used in any dynamic response calculation, should account for the *total* damping, which includes primarily a structural component, dependent on all the parameters noted above, and a (usually) lesser aerodynamic component, caused by the relative velocity of the building through the air. The aerodynamic contribution to damping should be negligible for those measurements performed under excitation by earthquakes or artificial means (such as mechanical shakers), but it may be significant when the excitation is ambient natural wind.

It is of interest to compare the low-level response data in Figs. 16 and 17 in terms of both the average conditions of all buildings, and a conservative value somewhat less than the average. The regression curves of damping vs. peak fluctuating displacement amplitude, for concrete buildings of 20 stories and greater, are compared in Fig. 19. The curves plotted with circles represent behavior based on the mean or expected value of damping. The box symbols labeled “m-s” represent a reduction of one standard deviation. Tamura proposes a low-amplitude range where damping increases quickly with drift, up to a threshold value of 2.5×10^{-5}. Above this limit no further increase is proposed—however, observations in this region were very scarce. The Davenport and Hill-Carroll curve is

* “Damping in Tall Buildings,” Unpublished report by Ove Arup & Partners, private communication.

shown as increasing throughout the plotted range, although it was derived from data apparently limited to a displacement amplitude of approximately $x/H = 3\times10^{-5}$ rms (Fig. 18) or about 10^{-4} peak.

The relevant range of drift amplitude in terms of acceleration for occupant comfort is indicated by the accessory scales at the top of the graph. The normalized amplitude range has been converted to peak amplitude by assuming a height of 3 m/floor, thence to peak acceleration by assuming a frequency of motion from Eq (1). The lowest end of interest is normally governed by human response to acceleration at a frequent (1 – 10 year) recurrence with typical criteria being 5 milli-g for perception, or 15 – 20 milli-g for comfort. In a 20-story building, for example, a peak acceleration of 20 milli-g corresponds to an amplitude of about 2×10^{-4} (1/5000). The upper end of interest is indicated by amplitudes from roughly 1/500 to 1/200. Note that the total drift—mean plus fluctuating peak—may differ from the amplitude (fluctuating peak) depending on the nature of the loading and response. For an along-wind response the total drift will be approximately twice the amplitude drift, and for a cross-wind response they will be about equal.

The heavy continuous line in Fig. 19 represents the average of Hill-Carroll's and Tamura's mean curves. The heavy broken line represents the average of the mean-minus-one-sigma curves. Traditionally, a curve reduced by 1 or even 2 sigma would be adopted by codes for design, to be conservative—at least for strength, if not performance. However, this would result in damping values that are well below those that have been traditionally used for many years, apparently with reasonable results. The authors propose that a damping curve corresponding to the mean expected value, represented by the heavy continuous line in Figure 19, should be considered for performance-based design of concrete buildings. For the ultimate limit state of say 500 to 1000 years recurrence (see below), where drift ratios would probably be just off the scale of available data, a maximum damping ratio of 0.025 is suggested. It should be noted that design deflections for ultimate wind loading should be less than those accepted for ultimate seismic limit states, as described in another paper, and the ultimate damping for wind should therefore be less than the value 0.05 that is generally accepted for seismic design.

Based on the above discussion, characteristic damping values associated with various limit states are summarized in Table 1. Additional work is obviously needed before specific values can be recommended for codification; however, it is proposed that the ranges shown represent reasonable limits. Within these ranges, additional consideration could or should address such parameters as building height, slenderness, and whether expected values (mean) or safe values (mean minus sigma) should be relied upon.

DESIGN RECURRENCE INTERVALS

Design values are related to various mean recurrence intervals, depending on the nature of the limit state under consideration. Common examples are:

Serviceability:	10-year recurrence
Nominal Strength:	50-year to 100-year recurrence
Ultimate strength:	500-year to 1000-year recurrence

In ASCE 7, ultimate design loads are approximated by multiplying the nominal strength design loads by a load factor. Nominal strength design loads are derived from nominal design wind speeds, which are defined as the ultimate wind speed divided by the square root of the load factor. The effective ultimate wind speed has a mean recurrence interval of approximately 720 years, and the load factor is 1.6, resulting in a nominal design wind speed having a mean recurrence of approximately 50 years.[*] This method can be inaccurate for dynamically active buildings, as shown below. The ASCE 7 committee is considering an ultimate wind speed map specifying speeds having a recurrence interval of 500 to 1000 years, with a load factor of unity.[†] Until a change of this nature is implemented, ultimate loads must be estimated through the present load factor approach.

For flexible buildings, can the 720-year load be obtained merely by multiplying the 50-year load by 1.6? Figure 20 suggests not. This is because the 1.6 load factor is based on the square of the ratio of the 720-year speed wind to the 50-year speed. This is acceptable for rigid buildings, but for flexible buildings the response load increases faster than wind speed squared due to the presence of resonance in the dynamic response. This is especially true in the crosswind direction, for reasons discussed above.

The results shown in Figure 20 are, however, for a constant value of, and we have just seen that damping increases with the level of response—and therefore with wind speed. If the rate of increase in damping were sufficient, this would counteract the increased dynamic resonant response sufficiently to coincide with the static response. Then the load factor of 1.6 would be justified in converting the 50-year load to a 720-year load. The required increase in damping to accomplish this can be determined analytically, based on typical measured slopes of the aerodynamic excitation spectra for alongwind and crosswind directions, e.g. from wind-tunnel measurements such as Fig. 9 or the online aerodynamic base moment database compiled by Zhou et al. (2003)(http://www.nd.edu/~nathaz).

---

[*] In most of the U.S. the resulting wind speed is exactly 50 years recurrence, but in hurricane-prone areas (where the rate of speed increase with recurrence is variable) the speed varies, typically between 50 and 100 years recurrence. In either case, the design speed may be referred to as the *nominal 50-year design speed*.

[†] Given the same nominal 50-year design speed, multiplication by √1.6 yields a 720-year speed, and multiplication by √1.53 yields a 500-year speed. The ASCE 7 committee determined that the load factor should be rounded to a single decimal, resulting in a load factor of 1.6.

Several results from the NATHAZ database are reproduced in Fig. 21. Although the spectra shapes and magnitudes vary considerably, they qualitatively resemble the spectra shown in Fig. 9, and within the most common range of reduced natural frequency, $0.1 < f_0B/U < 0.5$, the slopes m of the aerodynamic excitation are remarkably similar within the along-wind and cross-wind groups. By virtue of the log-log axes, this can be expressed as

$$\frac{f_0 S(f)}{\sigma_M^2} \propto \left(\frac{f_0 B}{U}\right)^m$$

or

$$f_0 S(f) \propto \left(\frac{f_0 B}{U}\right)^m U^2$$

where m takes on one characteristic value in the along-wind direction and a different characteristic value in the cross-wind direction. Using equation (17), the resonant portion of the response load can be expressed as

$$\mathbf{P}_R = C\zeta^{-1/2} f_0^{m/2} U^{-m/2} U^2 \tag{21}$$

where C is a constant. While this equation is interesting in itself in showing how the resonant load varies with damping, natural frequency, and wind speed, its more relevant use in the present context is to examine the interaction between damping and speed. If the total load $\mathbf{P}$ is to vary as U^2 (to justify the load factor approach), then the resonant portion must also vary as U^2 (noting that the mean and background portions inherently vary as U^2). If we assume that f_0 is constant, then the required variation of damping with wind speed is

$$\zeta(U) = DU^{-m} \tag{22}$$

where D is a constant, resulting in

$$\mathbf{P}_R = CDf_0 U^2 \tag{23}$$

as required. Now assume U_1 and U_2 are two wind speeds, associated with static loads P_1 and P_2 defined by a load factor F, which we also wish to apply to the dynamic response loads:

$$\frac{\mathbf{P}_{2,R}}{\mathbf{P}_{1,R}} \propto \frac{P_2}{P_1} = F \qquad \text{and} \qquad \frac{U_2}{U_1} = \sqrt{F} \tag{24}$$

The damping ratios corresponding to any two such speeds or loads, from equation (22), must satisfy

$$\frac{\zeta_2}{\zeta_1} = \left(\frac{U_2}{U_1}\right)^{-m} = F^{-m/2} \tag{25}$$

Consider for example the ASCE 7 case above where U_1 and $\mathbf{P}_1$ are the nominal 50-year speed and load, $F = 1.6$ is the load factor, and U_2 and $\mathbf{P}_2$ are the 720-year speed and load. Given the approximate slopes m from Fig. 21, the required damping ratios must satisfy

Along-wind: $m = -1.5$ $$\frac{\zeta_2}{\zeta_1} = 1.6^{1.5/2} = 1.42 \tag{26a}$$

Cross-wind: $m = -2.4$ $$\frac{\zeta_2}{\zeta_1} = 1.6^{2.4/2} = 1.76 \tag{26b}$$

Based on the results of the previous section, damping increases of this magnitude cannot generally be justified. If the structure's natural frequency is also considered variable (as it should be in a concrete building, given the variable state of cracking), say $f_0(U) \propto U^n$ with $n < 0$ as indicated in the left side of Fig. 15, then the requirement on ζ_2/ζ_1 would be even more severe. Wind tunnel tests show that the true load factor F can be slightly less than 1.6 for common along-wind cases, but greater than 1.6 in common cases where the resonant response is highly influenced by speed-dependent dynamic excitation such as vortex shedding or buffeting in the turbulent wake of an upwind building.

It must be noted that the above analysis is approximate and applies quantitatively only to regular rectangular building shapes in a regular uniform environment devoid of individual nearby interfering objects, and having a reduced natural frequency f_0D/U within the limits stated. The latter requirement can be exceeded for very tall buildings (low f_0), very slender buildings (low B), or extremely high or low wind speeds (U). In addition, the analysis applies only to the resonant portion of the total load, and is thus more significant to a cross-wind response (which can be almost entirely resonant) than to an along-wind response (where typically half or more of the total load is mean and background). Most practical buildings in their real surroundings are observed to behave within the approximate limits of equation (26).

This analysis reinforces the desirability of evaluating loads using the specific wind speeds and structural properties appropriate to the desired limit state, as opposed to the present practice of evaluating the loads using nominal 50-year-recurrence winds and properties and then multiplying by a "fits all" load factor.

SUMMARY AND CONCLUSIONS

This paper has presented the general state-of-the-art for understanding the dynamic response of building structures to wind. The important concepts include mean, background, and resonant response; spectral analysis; and static-equivalent loads. Examples were shown of simple generic buildings that illustrate the extreme cases of "pure" along-wind and cross-wind response. This background is necessary to describe the relevance of the structure's dynamic properties of natural frequency and damping ratio, particularly their variability as the wind speed varies over a wide range. Damping values were suggested for a range of limit states. In the context of performance-based design of building structures, an important conclusion is that the traditional load factor approach cannot be relied upon to produce accurate loads for different limit states.

REFERENCES

ASCE 7-05 (2006), *Minimum Design Loads for Buildings and Other Structures*, American Society of Civil Engineers, Reston, Virginia.

Blevins, R.D., 1990, *Flow-Induced Vibration*, Van Nostrand Reinhold, New York, pp. 330 – 331.

Boggs, D.W.; Hosoya, N.; and Cochran, L., 2000, "Sources of Torsional Wind Loading on Tall Buildings: Lessons From the Wind Tunnel," *Advanced Technology in Structural Engineering* (Proceedings of the 2000 Structures Congress & Exposition), ed. M. Elgaaly, SEI/ASCE.

Boggs, D.W. and Peterka, J.A., 1989, "Aerodynamic Model Tests of Tall Buildings, *Journal of Engineering Mechanics*, American Society of Civil Engineers, Vol. 115, No. 3, pp. 618 – 635.

Davenport, A.G., 1964, "Note on the Distribution of the Largest Value of a Random Function with Application to Gust Loading," *Proceedings of the Institution of Civil Engineers*, Vol. 28, June, pp. 187 – 196.

Davenport, A.G., 1966, "The Treatment of Wind Loading on Tall Buildings," Proceedings of a Symposium on Tall Buildings, University of Southampton, pp. 3 – 45.

Davenport, A.G., 1967, "Gust Loading Factors," *Journal of the Structural Division*, Proceedings of the American Society of Civil Engineers, Vol. 93, No. ST3, pp. 11 – 34.

Davenport, A.G. and Hill-Carroll, P., 1986, "Damping in Tall Buildings: Its Variability and Treatment in Design," *Building Motion in Wind*, ed. N. Isyumov and Tony Tschanz, American Society of Civil Engineers.

Tamura, Y.; Shimada, K.; Sasaki, A.; Kohsaka, R.; and Fujii, K, 1995, "Variation of Structural Damping Ratios and Natural Frequencies of Tall Buildings During Strong Winds," *Wind Engineering—Retrospect and Prospect* (Proceedings of the 9th International Conference on Wind Engineering), New Age International Publishers Limited, New Delhi.

Tamura, Y.; Suda, K.; and Sasaki, A., 2000, "Damping in Buildings for Wind Resistant Design," *International Symposium on Wind and Structures for the 21st Century*, Cheju, Korea, pp. 115 – 130.

Zhou, Y.; Kijewski, T; and Kareem, A., 2003, "Aerodynamic Loads on Tall Buildings: An Interactive Database," *Journal of Structural Engineering*, ASCE, Vol. 129, No. 3, pp. 394-404.

Table 1 – Characteristic Damping Values for Performance-Based Design of Concrete Buildings.
(Based on 20 stories minimum height

Limit state	Amplitude (assumed 1/2 total drift)	Recurrence interval	Critical damping ratio	
			Based on expected value	Based on expected value less one-sigma
Serviceability for occupant comfort under wind-induced motion	1×10^{-4} to 3×10^{-4} (Note 1)	10 years	0.016	0.010
Serviceability for drift	1.125×10^{-3} (1/800) (Note 2)	10 years	0.020	0.013
Traditional strength design	3×10^{-3} (1/400) (Note 3)	50 years	0.023	0.015
Ultimate strength	5×10^{-3} (1/200) (Note 4)	720 years	0.025	0.016

Note 1: Approximately 15 to 20 milli-g peak acceleration, depending on building height.
Note 2: Believed to be Committee consensus for "standard" 10-year drift criteria (1/400, = 2 × amplitude).
Note 3: Approximately 2 × 10-year value, based on 50-year speed / 10-year speed × uncracked section properties / cracked section properties (= 10-year value × 1.83 × 1.43).
Note 4: Approximately 1.6 × 50-year value, based on 720-year speed / 50-year speed.

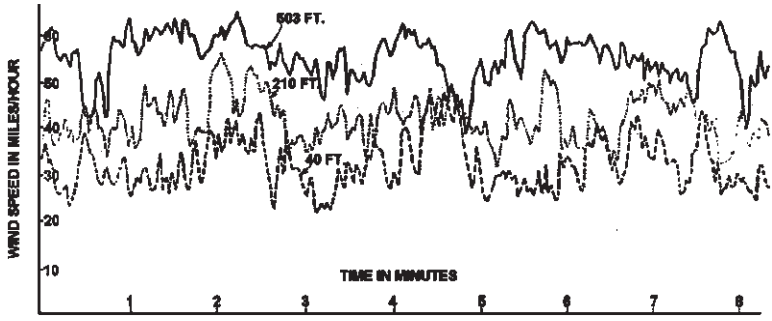

Figure 1 — Wind speeds at three heights on a 500-ft mast (Davenport 1966, 1967).

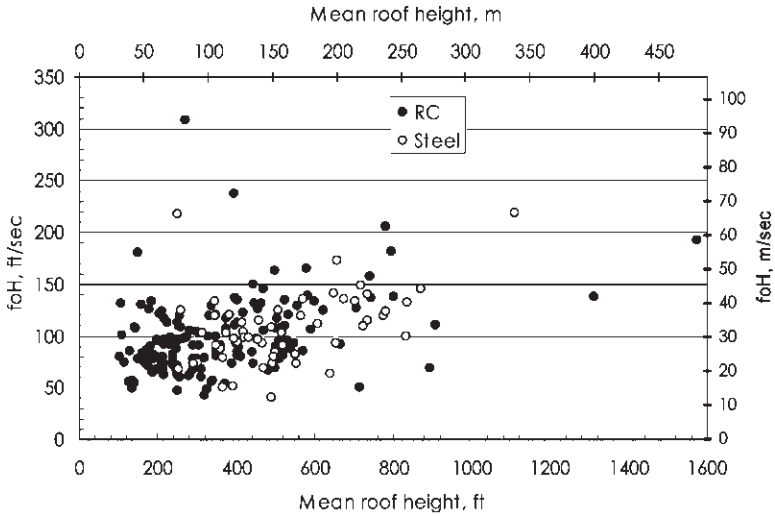

Figure 2 — Lowest natural frequency of many tall buildings as computed by design engineer (courtesy Cermak Peterka Petersen, Inc.).

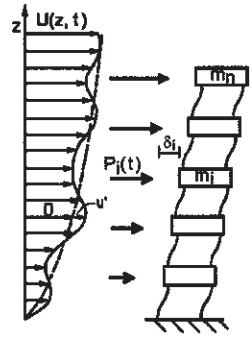

Figure 3 — Schematic of dynamic wind action on a building structure.

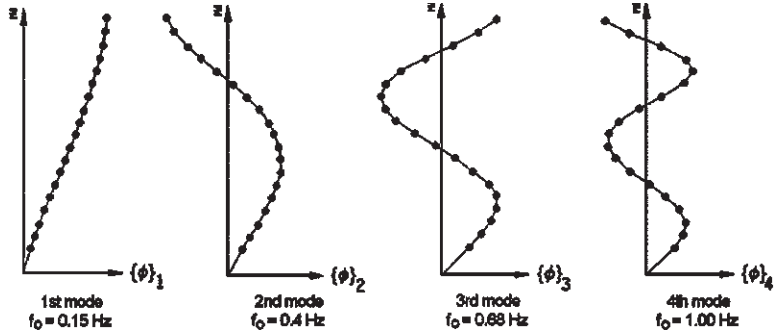

Figure 4 — Typical shapes and frequencies of the first few modes for a 20-story building structure.

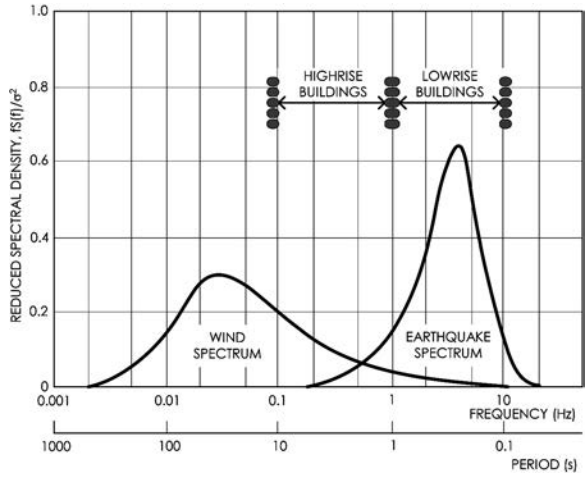

Figure 5 — Frequency range of structures excited by wind and earthquakes.

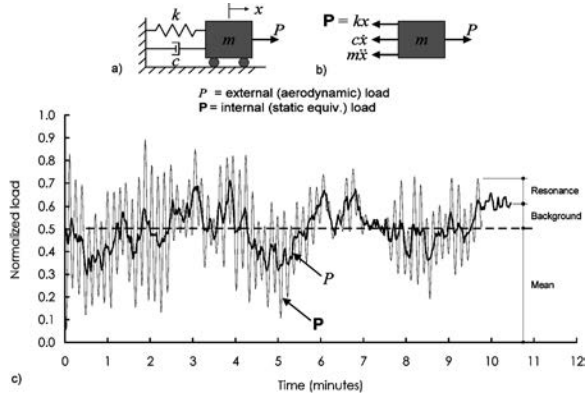

Figure 6 — Dynamic response of an SDOF system: (a) idealized system; (b) free-body diagram showing balance of forces; and (c) sample excitation and response.

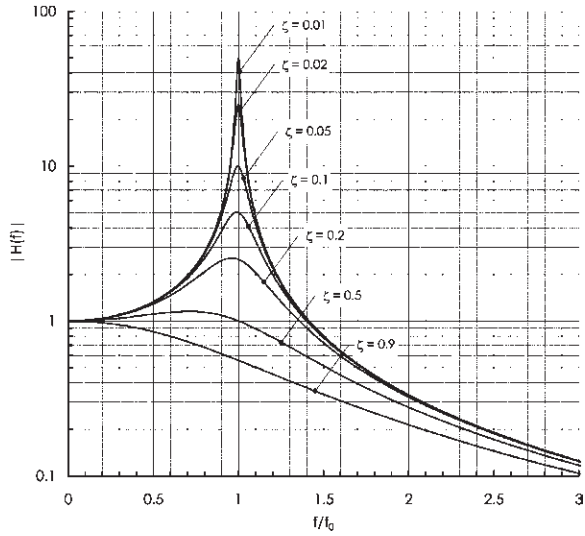

Figure 7 — SDOF dynamic amplification factor.

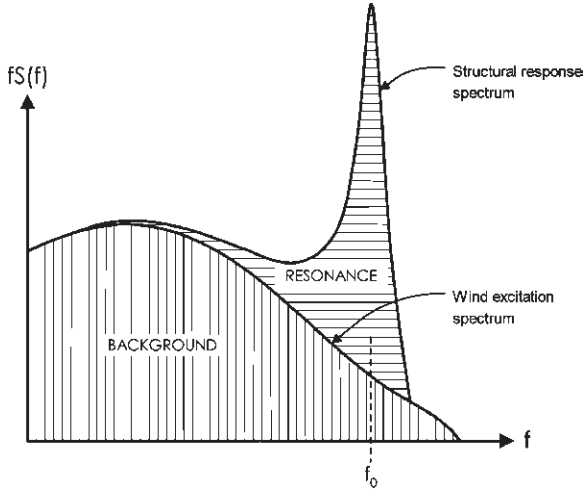

Figure 8 — Background and resonance contributions to response spectrum.

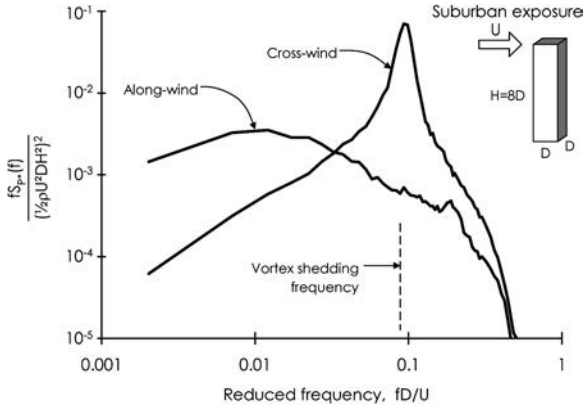

Figure 9 — Aerodynamic load spectra measured on a wind-tunnel model.

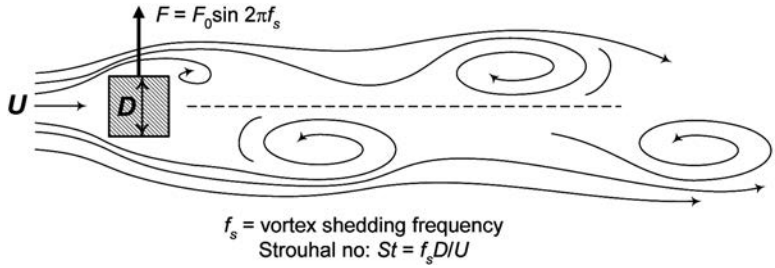

Figure 10 — Vortex shedding.

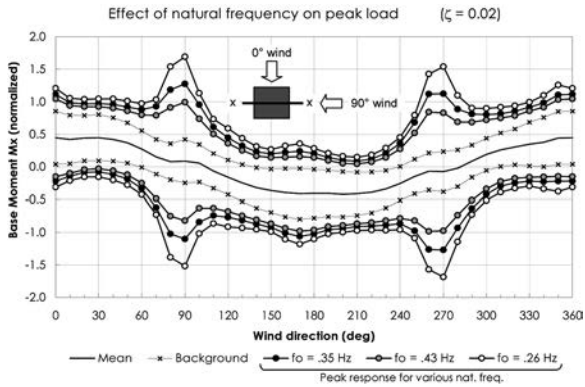

Figure 11 — Response base moment for a tall isolated flexible building showing the influence of natural frequency.

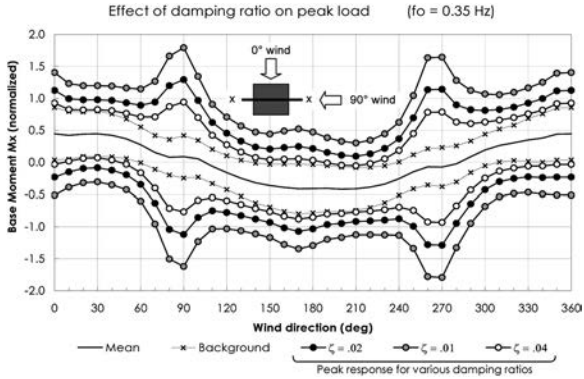

Figure 12 — Response base moment for a tall, isolated, flexible building showing effect of damping ratio.

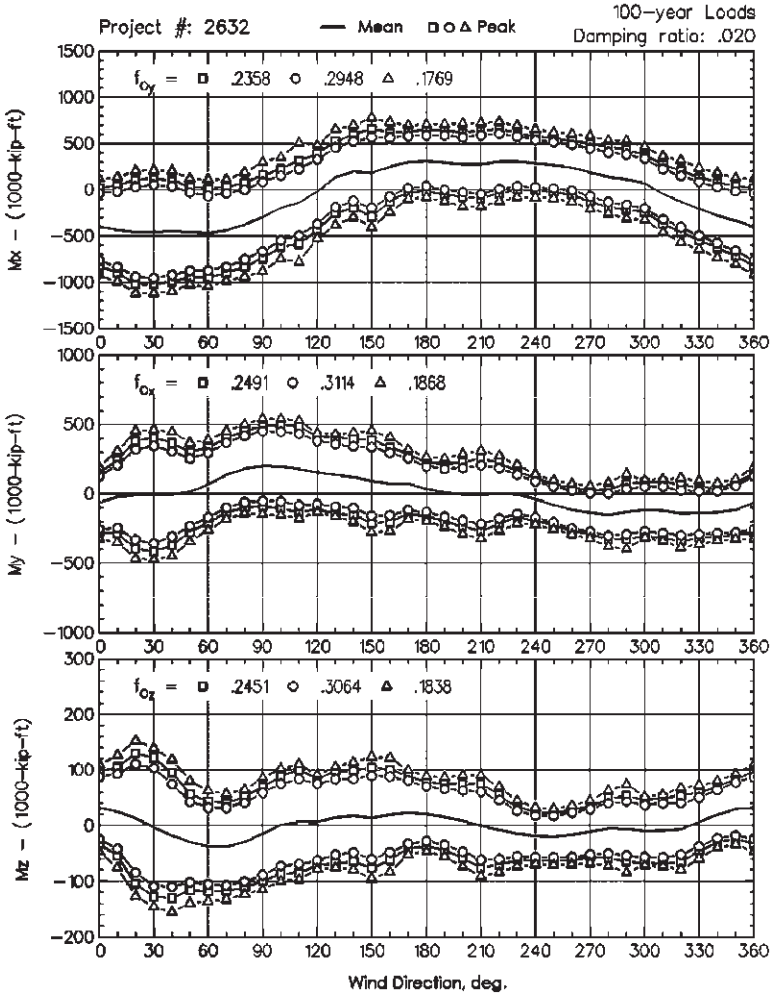

Figure 13 — Base response loads in all three components and all wind directions.

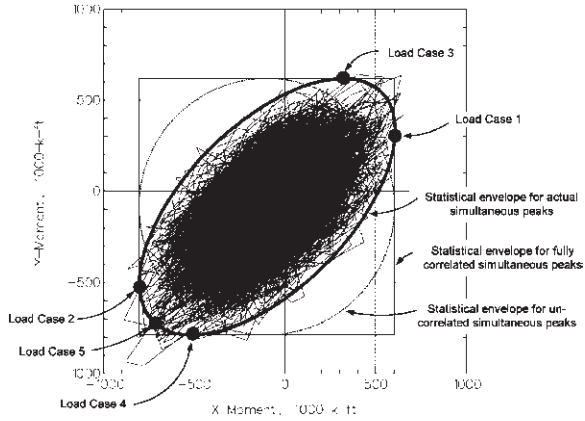

Figure 14 — Simultaneous response of two base moment components.

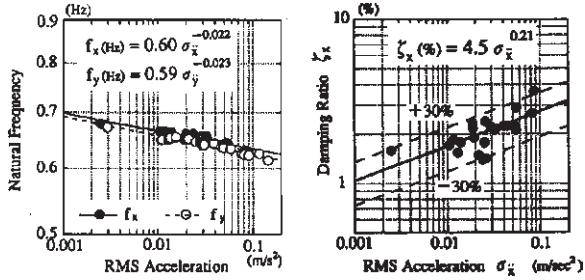

Figure 15 — Variation of natural frequency and damping ratio with level of response in a concrete tower (Tamura et al. 1995).

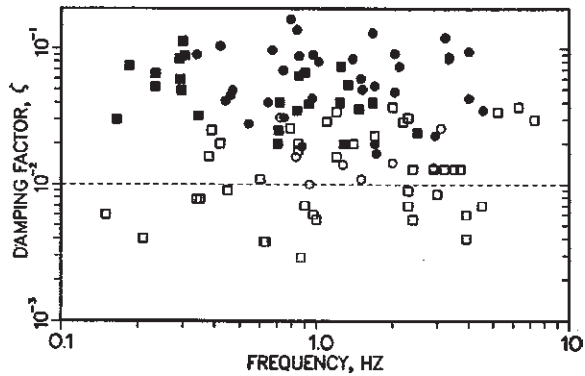

Figure 16 — Measured damping in California buildings. Circles = concrete; squares = steel; open = low-level excitation; filled = earthquake excitation (Blevins 1990).

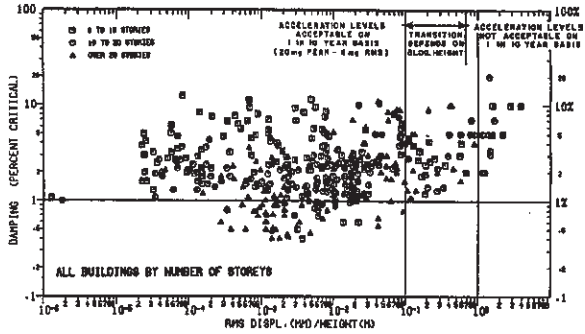

Figure 17 — Summary of damping estimates by amplitude of vibration by Davenport and Hill-Carroll (1986).

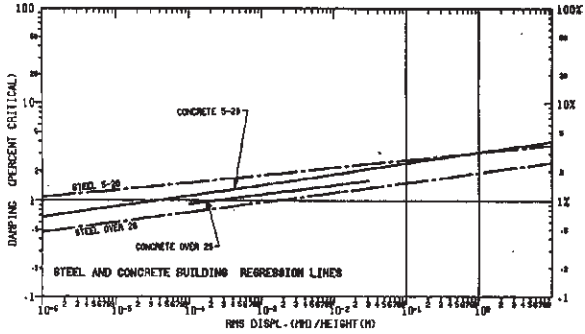

Figure 18 — Regression lines of damping by amplitude for steel and concrete buildings by Davenport and Hill-Carroll.

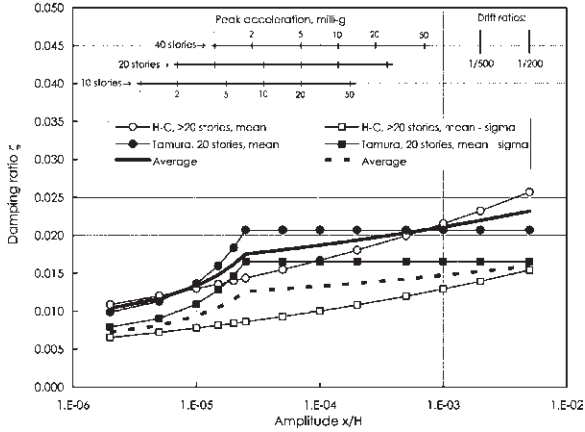

Figure 19 — Summary of damping prediction curves by Hill-Carroll (H-C) and Tamura.

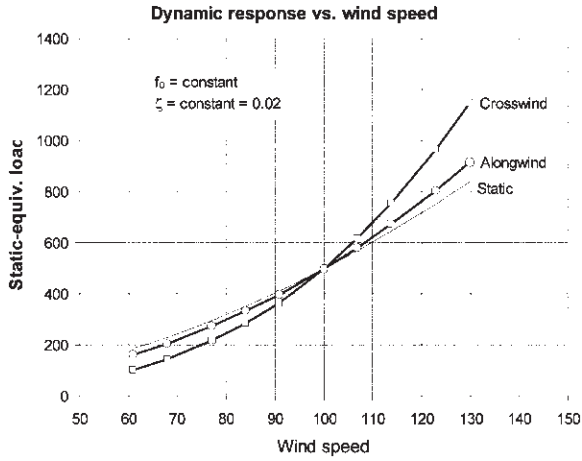

Figure 20 — Effective load versus wind speed for example rigid (static) and flexible buildings under along-wind and cross-wind response.

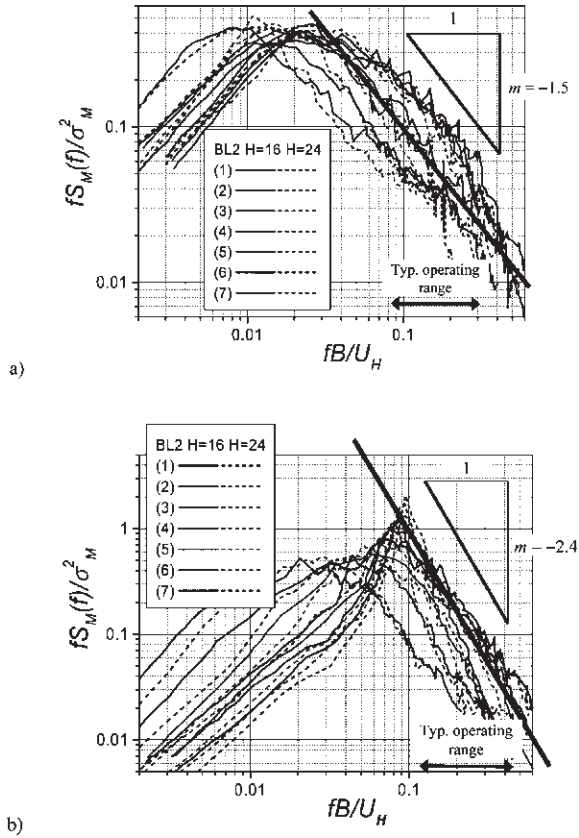

Figure 21 — Load spectra from the NATHAZ database for seven cross-section shapes in an urban boundary layer (Zhou et al 2003): (a) along-wind; and (b) cross-wind. Figures have been annotated to show the characteristic slope *m* applicable to the most common portion of the reduced frequency range.